

Exchange-enhanced photoelastic interaction and Bragg light diffraction by sound in antiferromagnets

E. A. Turov

Institute of the Physics of Metals, Ural Division of the USSR Academy of Sciences

(Received 27 February 1990)

Zh. Eksp. Teor. Fiz. **98**, 655–667 (August 1990)

Photoelastic interaction (PEI) associated with antiferromagnetism in such “easy-plane” trigonal antiferromagnetic crystals as α -Fe₂O₃ and FeBO₃ is investigated. It is demonstrated that due to exchange enhancement this antiferromagnetic magnetoelastic contribution to PEI may be comparable to or even exceed the values for the ordinary nonmagnetic PEI mechanism in crystals employed in acousto-optic devices. Light diffraction by sound under Bragg conditions is calculated for such PEI and it is shown that a magnetic field can control both the Bragg angle and the diffracted light intensity. Specific quantitative estimates of the effects are produced for α -Fe₂O₃ and FeBO₃ in their corresponding transparency regions.

1. INTRODUCTION

Photoelastic interaction^{1,2} PEI can be defined as an elastic stress-induced change in the permittivity, $\Delta\varepsilon_{\alpha\beta}$. Ordinarily for magnetically disordered crystals we have

$$\Delta\varepsilon_{\alpha\beta} = P_{(\alpha\beta)(\gamma\delta)} e_{\gamma\delta} + P_{[\alpha\beta][\gamma\delta]} \omega_{\gamma\delta}, \quad (1)$$

where

$$e_{\alpha\beta} = (\partial u_\alpha / \partial x_\beta + \partial u_\beta / \partial x_\alpha) / 2, \quad \omega_{\alpha\beta} = (\partial u_\alpha / \partial x_\beta - \partial u_\beta / \partial x_\alpha) / 2$$

are the strain and local rotation tensors, respectively; $P_{\alpha\beta\gamma\delta}$ is the PEI tensor; and the tensor is symmetrical in the indices in parentheses in (1), and is antisymmetrical in the indices in brackets.

Antiferromagnetics have an additional PEI associated with the antiferromagnetism vector

$$\mathbf{L} = 2M_0 \mathbf{l} = \mathbf{M}_1 - \mathbf{M}_2 \quad (2)$$

and, to a lesser degree, the magnetization vector

$$\mathbf{M} = 2M_0 \mathbf{m} = \mathbf{M}_1 + \mathbf{M}_2 \quad (3)$$

(\mathbf{M}_1 and \mathbf{M}_2 are the sublattice magnetizations). This antiferromagnetic PEI is most easily obtained directly from the antiferromagnetic part of the tensor $\varepsilon_{\alpha\beta}$ ^{3,4}

$$\varepsilon_{\alpha\beta}^L = ia_{\alpha\beta\gamma} l_\gamma + b_{\alpha\beta\gamma\delta} l_\gamma l_\delta + c_{\alpha\beta\gamma\delta} h_\gamma l_\delta, \quad (4)$$

(where $\mathbf{H} = 2M_0 \mathbf{h}$ is the magnetic field), if we find the sound-induced variations $\delta \mathbf{l}(e_{\alpha\beta}, \omega_{\alpha\beta})$.

Sound will induce rotations of the vectors \mathbf{L} and \mathbf{M} in this plane (Fig. 1) by some angle $\delta\varphi(e_{\alpha\beta}, \omega_{\gamma\delta})$ in “easy plane” antiferromagnetics (EPA). In view of the small anisotropy in the easy plane the entire system of \mathbf{L} and \mathbf{M} will in fact be constrained from rotation in this plane by the field \mathbf{H} due to the low magnetization $M = M_0 H / H_E$ (H_E is the effective homogeneous exchange field), which is facilitated by the energy $M_0 H (H / H_E)$. At the same time the stresses $e_{\alpha\beta}$ (and $\omega_{\alpha\beta}$), due to the magnetoelastic bonding energy $B l_\alpha l_\beta e_{\gamma\delta} \approx B e_{\gamma\delta}$ (B is the magnetostriction constant) act through the vector \mathbf{L} whose modulus $L \approx 2M_0 \gg M$. As a result the angle of rotation

$$\delta\varphi \approx -l_x \approx \frac{B}{MH} e_{\gamma\delta} \approx \frac{B}{M_0 H} \left(\frac{H_E}{H} \right) e_{\gamma\delta} \quad (5)$$

contains an additional large multiplier H_E / H here com-

pared to the corresponding expression for the ferromagnet. This also is the cause of so-called exchange enhancement of magnetoelastic effects in EPA.

We note that the angle $\delta\varphi$ given by Eq. (5) may become of order 1 rad under stresses as low as $e_{\gamma\delta} \approx 10^{-5}$. This means that the antiferromagnetic PEI $\Delta\varepsilon^L(e_{\alpha\beta}, \omega_{\alpha\beta})$ will in this case approach the maximum possible value $\Delta\varepsilon_{\alpha\beta}^L \approx \varepsilon_{\alpha\beta}^L$, which, as we shall see below, is not only comparable to but will even exceed the ordinary crystalloelectric PEI in nonmagnetic crystals used in acousto-optic devices. Here one particular fact of special interest for acousto-optics is that antiferromagnet PEI may be heavily dependent on the magnetic field H [which is already evident from (5)].

We note that since $\varepsilon_{\alpha\beta}^L$, defined by Eq. (4), contains terms linear in \mathbf{L} that are responsible for the antiferromagnetic Faraday effect,⁴ the contribution to PEI resulting from $\varepsilon_{\alpha\beta}^L$ will contain, along with terms of the type in Eq. (1), additional terms of the form

$$P_{[\alpha\beta](\gamma\delta)} e_{\gamma\delta} + P_{[\alpha\beta][\gamma\delta]} \omega_{\gamma\delta}. \quad (6)$$

The PEI exchange enhancement effect in EPA was first predicted in Ref. 5, which also identified by experiment the associated acoustic light modulation.

The present paper is designed to carry out a detailed examination of the PEI antiferromagnetic tensor for trigonal EPAs (with the $\bar{1}+3+2^-$ structure)⁴ and to use this as the basis for calculating light diffraction by sound. Here

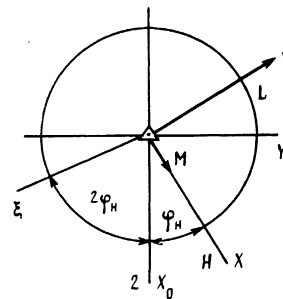


FIG. 1. The various coordinate axes selected in the basal plane: The X_0 axis runs along axis of symmetry 2: ($Y_0 \perp X_0$); The axis runs along the field H at angle H to X_0 ($L \parallel Y$); ξ is the direction of the polarization vector \mathbf{u} of a soft transverse acoustic mode with $q \parallel Z$ [3^+ [its velocity is given by Eqs. (30)].

the discussion will concern so-called Bragg diffraction conditions, i.e., under the condition

$$d \gg n\Lambda^2/2\pi\lambda_0, \quad (7)$$

where d is the optical path length of the acoustic beam, while Λ and λ_0/n is the wavelength of sound and light, respectively (n is the refractive index). This condition derives from the requirement that the light beam intersect a sufficiently large number of acoustic wavefronts.¹ It is Bragg light diffraction by sound that is widely and effectively used in acousto-optic electronic devices.^{1,2}

In order to stimulate interest on the part of experimental researchers in acousto-optic phenomena in antiferromagnetics we consider a number of different geometrical situations with respect to the relative configuration of the wave vectors and light and sound polarizations as well as magnetic field directions and crystal axes of symmetry. This will permit selection of an optimum experimental geometry. In addition to describing qualitative behavior the present study will also derive quantitative estimates of these effects in all cases where possible.

2. PHOTOELASTIC INTERACTION TENSOR

Following the outline described above for obtaining antiferromagnetic PEI we write the explicit form of the components of the complete permittivity vector $\bar{\epsilon}_{\alpha\beta}$ accounting for the antiferromagnetic terms of Eq. (4) for an $\bar{1}+3+2^-$ structure EPA, using $Z \parallel 3^+$, $X \parallel \mathbf{M}^{(0)}$, \mathbf{H} , and $Y \parallel \mathbf{L}^{(0)}$ as the coordinate axes (Fig. 1), where $\mathbf{M}^{(0)}$ and $\mathbf{L}^{(0)}$ are the equilibrium magnetization and antiferromagnetism vectors, respectively. A system with an $X_0 \parallel 2^-$ axis will also be used as an alternative system, the first system is rotated by φ_H about the 3^+ axis relative to the second system. In the X, Y, Z coordinate system we have

$$\bar{\epsilon}_{xx} = \epsilon_0 + b_2 l_y^2 + c_1 h_x l_y, \quad (8)$$

$$\bar{\epsilon}_{yy} = \epsilon_0 + b_1 l_y^2 - c_2 h_x l_y, \quad (9)$$

$$\bar{\epsilon}_{zz} = \epsilon_0 + c_4 h_x l_y, \quad (9)$$

$$\left. \begin{aligned} \bar{\epsilon}_{(xy)} &\equiv \bar{\epsilon}_{(xy)}^L = (b_1 - b_2) l_x l_y - \frac{1}{2} (c_1 + c_2) h_x l_x, \\ \bar{\epsilon}_{(xz)} &\equiv \bar{\epsilon}_{(xz)}^L = b_3 [(l_x^2 - l_y^2) \sin 3\varphi_H + 2l_x l_y \cos 3\varphi_H] \\ &\quad + c_3 h_x (l_y \sin 3\varphi_H - l_x \cos 3\varphi_H), \end{aligned} \right\} \quad (10)$$

$$\left. \begin{aligned} \bar{\epsilon}_{(yz)} &\equiv \bar{\epsilon}_{(yz)}^L = b_3 [(l_x^2 - l_y^2) \cos 3\varphi_H - 2l_x l_y \sin 3\varphi_H] \\ &\quad + c_3 h_x (l_y \cos 3\varphi_H + l_x \sin 3\varphi_H), \end{aligned} \right\} \quad (11)$$

$$\bar{\epsilon}_{[xy]} \equiv \bar{\epsilon}_{[xy]}^L = 0, \quad (12)$$

$$\bar{\epsilon}_{[xz]} \equiv \bar{\epsilon}_{[xz]}^L = -ial_x, \quad \bar{\epsilon}_{[yz]} \equiv \bar{\epsilon}_{[yz]}^L = -ial_y. \quad (13)$$

Here $l_z = 0$ and $h_x = H/2M_0$ are used.

It is now necessary to account for sound-induced oscillations of \mathbf{l} in Eqs. (8)–(13): $\delta\mathbf{l} = \delta\mathbf{l}(e_{\alpha\beta}, \omega_{\alpha\beta})$. We consider the acoustic frequencies

$$\Omega \ll \omega_{\text{AFRF}}, \quad (14)$$

where ω_{AFRF} is the antiferromagnetic resonance frequency (AFRF) for its low frequency (quasiferromagnetic) mode.⁶ Here $\delta\mathbf{l}$ can be found by minimizing the sum of the magnetic and magnetoelastic energies. The result, which sharpens Eq. (5), is as follows:^{4,7}

$$\begin{aligned} \delta l_x \equiv l_x \approx -\delta\varphi = -\frac{H_E}{M_0 H_{e1}^2} [2B_{66} e_{xy} \\ + 4B_{14} (e_{xz} \cos 3\varphi_H - e_{yz} \sin 3\varphi_H)], \end{aligned} \quad (15)$$

$$l_y \approx 1, \quad l_z = 0,$$

where $B_{00} \equiv B_{11} - B_{12}$ and B_{14} are the magnetostriction constants, while

$$H_{e1}^2 = \omega_{\text{AFRF}}/\gamma^2 = H(H + H_D) + H_{\Delta}^2 \quad (16)$$

is the quantity determining the AFRF frequency figuring in Eq. (14). In Eq. (16) H_D is the Dzyaloshinskii field responsible for weak ferromagnetism, while H_{Δ}^2 accounts for the contributions of magnetic anisotropy in the XY plane as well as magnetoelastic and hyperfine interaction to ω_{AFRF} . We note that there are no terms with δl_x in $\omega_{\alpha\beta}$ as given by (15). In this case they may be discarded, given the smallness of trigonal magnetic anisotropy which would produce such terms.

Substitution of $\mathbf{l} = \mathbf{l}^{(0)} + \delta\mathbf{l}$ into $\bar{\epsilon}_{\alpha\beta}$ of Eqs. (8)–(13) decomposes the tensor $\hat{\epsilon}$ into its equilibrium part $\hat{\epsilon}$ and photoelastic interaction $\Delta\hat{\epsilon}$:

$$\hat{\epsilon} = \hat{\epsilon} + \Delta\hat{\epsilon}.$$

The components of the tensor $\hat{\epsilon}$ in the geometry shown in Fig. 1 are as follows. The diagonal components are

$$\begin{aligned} \epsilon_{xx} &\equiv n_{xx}^2 = \epsilon_0 + b_2 l_y^2 + c_1 h_x l_y, \\ \epsilon_{yy} &\equiv n_{yy}^2 = \epsilon_0 + b_1 l_y^2 - c_2 h_x l_y, \\ \epsilon_{zz} &\equiv n_{zz}^2 = \epsilon_0 + c_4 h_x l_y; \end{aligned} \quad (17)$$

and the nondiagonal components are

$$\begin{aligned} \epsilon_{yx} &= \epsilon_{xy} = 0, \\ \epsilon_{zx} &= \epsilon_{xz} = (-b_3 l_y^2 + c_3 h_x l_y) \sin 3\varphi_H, \\ \epsilon_{yz} &= (-b_3 l_y^2 + c_3 h_x l_y) \cos 3\varphi_H - ial_y, \\ \epsilon_{zy} &= (-b_3 l_y^2 + c_3 h_x l_y) \cos 3\varphi_H + ial_y \end{aligned} \quad (18)$$

(here $l_y = 1$ is retained solely to denote the antiferromagnetic origin of the individual terms). The components of the photoelastic part $\Delta\hat{\epsilon}$ can be represented as expressions similar to Eq. (1) subject to Eq. (6) in which the coefficients $P_{\alpha\beta\gamma\delta}$ —the PEI tensor components—can be given in the following specific form:

$$\left. \begin{aligned} P_{(xy)(xy)} &= U_1 \Pi_1, \\ P_{(xy)(xz)}/\cos 3\varphi_H &= -P_{(xy)(yz)}/\sin 3\varphi_H = U_2 \Pi_1, \end{aligned} \right\} \quad (19)$$

$$P_{(xz)(xy)}/\cos 3\varphi_H = -P_{(yz)(xy)}/\sin 3\varphi_H = U_1 \Pi_2, \quad (20)$$

$$\begin{aligned} P_{(xz)(xz)}/2 \cos^2 3\varphi_H &= -P_{(yz)(yz)}/2 \sin^2 3\varphi_H = -P_{(xz)(yz)}/\sin 6\varphi_H \\ &= P_{(yz)(xz)}/\sin 6\varphi_H = -U_2 \Pi_2, \end{aligned} \quad (21)$$

$$P_{[xz](xy)} = U_1 (ial_y) \equiv U_1 \epsilon_{[zy]}, \quad (22)$$

$$P_{xz}/\cos 3\varphi_H = -P_{[xz](yz)}/\sin 3\varphi_H = U_2 (ial_y) \equiv U_2 \epsilon_{[zy]}, \quad (23)$$

$$P_{[xz][xy]} = -P_{[xy][xz]} = ial_y \equiv \epsilon_{[zy]}, \quad (24)$$

where

$$U_1 = \frac{B_{66} H_E}{M_0 H_{e1}^2}, \quad U_2 = \frac{2B_{14} H_E}{M_0 H_{e1}^2}, \quad (25)$$

$$\Pi_1 = (b_1 - b_2) l_y^{-1/2} (c_1 + c_2) h_x l_y, \quad \Pi_2 = -b_3 l_y^{2+1/2} c_3 h_x l_y. \quad (26)$$

The components of the tensor \hat{P} in Eqs. (19)–(23) are expressed as products of two factors. The first factors (U_1 or U_2) are purely of magnetoelastic origin and their values are well known from magnetoacoustics for the antiferromagnets of interest to us. The second factors (Π_1 or Π_2) are determined through antiferromagnetic permittivity terms (17), (18). Unfortunately the experimental data for these terms from magneto-optic experiments are quite sparse. Nonetheless we will use these data in Section 4 when we will apply general formulae to specific antiferromagnets. In the interim we note that

$$\Pi_1 \approx \begin{cases} \varepsilon_{yy} - \varepsilon_{xx} & \text{as } H \rightarrow 0, \\ \frac{1}{2}(\varepsilon_{yy} - \varepsilon_{xx}) & \text{as } H \rightarrow \infty, \end{cases} \quad (27)$$

$$\Pi_2 \approx \begin{cases} \varepsilon_{(xz)}|_{\varphi_H = \pi/2} & \text{as } H \rightarrow 0, \\ \frac{1}{2} \varepsilon_{(xz)}|_{\varphi_H = \pi/2} & \text{as } H \rightarrow \infty. \end{cases} \quad (28)$$

The expression for $U_{1,2}$ in (25) can be treated as antiferromagnetic PEI enhancement factors. Indeed ordinarily the PEI tensor components are roughly of the same order as the anisotropy of the tensor $\varepsilon_{\alpha\beta}$. In any case this will definitely occur for the rotation components of the tensors \hat{P} [the second term in Eqs. (1) and (6)] due to the local rotations $\omega_{\alpha\beta}$ of the crystal volume elements (with their crystallographic axes). This also applies to antiferromagnetic PEI in the part related to acoustical rotations of the volume elements. The latter is clear from Eq. (24), which provides sample components of the tensor \hat{P} attributable specifically to such rotations: No enhancement occurs in this case. The exchange-enhanced components of the tensor \hat{P} in Eqs. (19)–(23) have an entirely different origin. They are caused by rotations of the vector \mathbf{L} and although the anisotropy of the tensor $\delta\varphi$ associated with \mathbf{L} is small compared to the crystallographic anisotropy of this tensor, the angle of rotation $\varepsilon_{\alpha\beta}$ in Eq. (15) is enormous. This is in fact responsible for the enhancement of $U_{1,2}$ in Eqs. (19)–(23).

The table provides the theoretical values of the coefficients U_1 and U_2 for α -Fe₂O₃ and FeBO₃ calculated using the parameters given in the Appendix (for near-room temperatures). Values sufficient to eliminate the domain structure were selected for the fields \mathbf{H} ; these fields are different for α -Fe₂O₃ and FeBO₃. The table also provides the components of the tensor \hat{P} that could be calculated using existing experimental data from magneto-optic experiments for antiferromagnetics: For α -Fe₂O₃ accounting for Eq. (27),

$\Pi_1 = 12 \cdot 10^{-4}$ (Ref. 3), while for FeBO₃ $\Pi_1 = 6.6 \cdot 10^{-4}$ (Ref. 8) while in Eq. (23) $\varepsilon_{[zy]}^L/i = a = 14 \cdot 10^{-4}$ (Ref. 9). Unfortunately experiments to determine $\varepsilon_{(xz)}^L$ which are required to estimate Π_2 in Eq. (28) and consequently the other components of the tensor \hat{P} , are not available. For comparison purposes the table provides the values of the same components of \hat{P} for materials used in acousto-optics, sapphire (Al₂O₃) and lithium niobate (LiNbO₃). The last row provide the wavelength of light λ_0 (in a vacuum) in the transparency range of these crystals.

It is necessary to explain the index ξ in $P_{(xy)(z\xi)}$ and $P_{[xz][z\xi]}$. The ξ and $\eta^1 \xi$ axes in the XY plane (rotated by $-3\varphi_H$ relative to the X and Y axes: See Fig. 1) determine the directions of the polarization vectors $\mathbf{u}_1 \parallel \xi$ and $\mathbf{u}_2 \parallel \eta$ for normal acoustic waves with wave vector $\mathbf{q} \parallel Z$ (Ref. 10). These correspond to the shear strains

$$\begin{aligned} e_{z\xi} &= e_{zx} \cos 3\varphi_H - e_{zy} \sin 3\varphi_H = e_{zx} \cos 2\varphi_H - e_{zy} \sin 2\varphi_H, \\ e_{z\eta} &= e_{zy} \cos 3\varphi_H + e_{zx} \sin 3\varphi_H = e_{zy} \cos 2\varphi_H + e_{zx} \sin 2\varphi_H. \end{aligned} \quad (29)$$

The corresponding components of the tensor \hat{P} are related in the second pair of indices by these same relations. Here $P_{(xy)(z\xi)}$ and $P_{(xz)(z\xi)}$ are maximized while $P_{(xy)(z\eta)} = P_{(xz)(z\eta)} = 0$. (The latter also applies to LiNbO₃ for which $\eta \equiv y_0$.) It is important that due to magnetoelastic interaction the velocities of these two transverse modes are different:

$$\begin{aligned} s_{(z\xi)}^2 &= v_1^2 \left(1 - \frac{2B_{14}}{C_{44}} U_2 \right), \\ s_{(z\eta)}^2 &= v_1^2 = C_{44}/\rho. \end{aligned} \quad (30)$$

Modes with $\mathbf{q} \parallel X$, $\mathbf{u} \parallel Y$ for $\cos 3\varphi_H = 0$ and with $\mathbf{q} \parallel Y$, $\mathbf{u} \parallel X$ for $\sin 3\varphi_H = 0$ are also pure normal modes. These have velocity

$$s_{(xy)}^2 = v_2^2 \left(1 - \frac{B_{66}}{C_{66}} U_1 \right), \quad v_2^2 = C_{66}/\rho. \quad (31)$$

The transverse waves with $\mathbf{u} \perp Z$ and $\mathbf{u} \parallel Z$ mix with other directions of \mathbf{q} and \mathbf{H} in the XY plane and may also include the longitudinal wave with $\mathbf{u} \parallel \mathbf{q}$.

We note the clear dependence of velocities (30) and (31) on \mathbf{H} (Ref. 11). With the values of \mathbf{H} shown in the table the second term in braces in Eq. (30) has a relative value of 25% and 6% for α -Fe₂O₃ and FeBO₃, respectively. However an even stronger relation of antiferromagnetic light diffraction by sound is directly manifested through the PEI tensor, in which, as we see from Eqs. (19)–(26), both factors are

TABLE I.

Parameter	α -Fe ₂ O ₃	FeBO ₃	Al ₂ O ₃	LiNbO ₃
H, ϑ	10 ³	10 ²	—	—
$U_1 \cdot 10^{-3}$	2.4	3.2	—	—
$U_2 \cdot 10^{-3}$	5.0	4.6	—	—
$P_{(xy)(xy)}$	2.8	2.1	1.0	0.82
$P_{(xy)(z\xi)}$	9.6	5.1	0.0	1.8*
$P_{[xz](xy)}$?	4.5	0	0
$P_{[xz](z\xi)}$?	6.5	0	0
λ_0, nm	1150	514.5	644	633

* $\xi \equiv x_0$.

functions of \mathbf{H} . This reveals that it is possible to some degree to control the diffracted light by altering the magnitude and direction of \mathbf{H} and also to modulate it by modulating \mathbf{H} .

3. GENERAL EQUATIONS FOR THE AMPLITUDES AND BRAGG ANGLES OF INCIDENT AND DIFFRACTED LIGHT

The problem of light diffraction by an elastic acoustic wave field is reduced to solving the equation¹

$$\Delta \mathbf{E} - \nabla(\nabla \mathbf{E}) - \frac{1}{c^2} \frac{\partial^2}{\partial t^2} (\hat{\epsilon} \mathbf{E}) = -\frac{1}{c^2} \frac{\partial^2}{\partial t^2} (\Delta \hat{\epsilon} \mathbf{E}), \quad (32)$$

where $\hat{\epsilon}$ is the permittivity tensor with components (17), (18), while $\Delta \hat{\epsilon}$ is its sound-induced perturbation with the components defined by Eq. (1) subject to Eq. (6) together with Eqs. (19)–(23) (we account for only the exchange-enhanced components of \hat{P}). Using the coupled mode method¹ we search the solution of Eq. (32) as a superposition of two natural optical modes corresponding to $\Delta \hat{\epsilon} = 0$:

$$\mathbf{E} = \sum_{j=1,2} A_j(\mathbf{r}) \mathbf{p}_j \exp[i(\mathbf{k}_j \mathbf{r} - \omega_j t)]. \quad (33)$$

One of these modes is an incident wave (of frequency ω_1 , wave vector \mathbf{k}_1 and a unitary polarization vector \mathbf{p}_1), while the second mode is a diffracted wave (ω_2 , \mathbf{k}_2 , \mathbf{p}_2); here the desired amplitudes of these waves $A_j(\mathbf{r})$ can be treated as slowly varying functions of the coordinates (due to smallness of $\Delta \hat{\epsilon}$).

As is ordinarily the case we consider only the cases of small (Fig. 2, a) and large (Fig. 2, b) Bragg angles (SBA and LBA), i.e., the angles formed by the vectors \mathbf{k}_1 and \mathbf{k}_2 with the wavefront of the acoustic wave. In Figs. 2, a and b, this will correspond to angles $\theta_{1,2}$ (SBA) and $\pi/2 - \theta_{1,2}$ (LBA), respectively. In both cases we use the condition

$$|\sin \theta_{1,2}| \ll 1, \quad (34)$$

which allows us to treat $A_j(\mathbf{r})$ as a function of only a single variable.

We focus primarily on two choices of the coordinate axes (A and B) attached to the sample (the Z axis is parallel to axis 3; the X axis is parallel to the field \mathbf{H} and forms an angle φ_H with axis 2, which is parallel to the X_0 axis while the Y axis is parallel to the vector \mathbf{L} : See Fig. 1) and fixed with respect to the direction of the wave vectors of light (\mathbf{k}_1 and \mathbf{k}_2) and sound (\mathbf{q}). This is reflected in the corresponding configuration of the coordinate axes: A (B) in Fig. 2, a and b.

Version A. When condition (34) holds the amplitudes

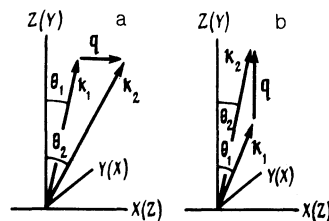


FIG. 2. Relative configuration of the wave vectors of the light (\mathbf{k}_1 and \mathbf{k}_2) and acoustic (\mathbf{q}) waves and the X , Y , Z coordinate axes (see Fig. 1) for the case of small Bragg angles (a) and large Bragg angles (b). Two versions are shown: A (without braces) and B (in braces); B is obtained from A by the cyclic substitution: $x \rightarrow z \rightarrow y \rightarrow x$. The text also considers version C obtained from B by the substitution: $z \rightarrow x$, $x \rightarrow -z$.

$A_j = A_j(z)$ are slowly varying functions of z , and if we assume that

$$\Delta \epsilon = \Delta \epsilon_0 \sin(\mathbf{q} \mathbf{r} - \Omega t)$$

($q \equiv q_x, 0, q_z$), then for the Bragg diffraction conditions (7) Eq. (32) together with Eq. (33) yields the following system neglecting the second derivatives of $A_j(z)$ with respect to z :

$$\begin{aligned} \pm \frac{\partial A_1}{\partial z} &= -\kappa_{12} \frac{\omega_1}{\omega_2} \left| \frac{k_{2z}}{k_{1z}} \right|^{1/2} (\text{sign } k_{1z}) A_2, \\ \pm \frac{\partial A_2}{\partial z} &= \kappa_{12} \frac{\omega_2}{\omega_1} \left| \frac{k_{1z}}{k_{2z}} \right|^{1/2} (\text{sign } k_{2z}) A_1, \end{aligned} \quad (35)$$

which is supplemented by the corresponding Bragg coherence conditions:

$$\begin{aligned} \omega_2 &= \omega_1 \pm \Omega, \\ \mathbf{k}_2 &= \mathbf{k}_1 \pm \mathbf{q}. \end{aligned} \quad (36)$$

In Eqs. (35)

$$\kappa_{12} = \kappa_{21} = \frac{\omega_1 \omega_2 (p_{1\alpha} \Delta \epsilon_{0\alpha\beta} p_{2\beta})}{4c^2 |k_{1z} k_{2z}|^{1/2}}, \quad (37)$$

where

$$\Delta \epsilon_{0\alpha\beta} = P_{\alpha\beta(\gamma\delta)} e_{\gamma\delta}^{(0)} + P_{\alpha\beta(\gamma\delta)} \omega_{\gamma\delta}^{(0)}, \quad (38)$$

while $e_{\gamma\delta}^{(0)}$ and $\omega_{\gamma\delta}^{(0)}$ are the amplitudes of the strain and local rotation tensors.

We note that k_1 and k_2 , which satisfy condition (36), are simultaneously eigennumbers of Eq. (32) for $\Delta \epsilon = 0$. For given values of θ_1 and θ_2 we find approximately

$$\begin{aligned} k_1 &= n_{vv} \frac{\omega_1}{c}, \\ k_2 &= n_{xx} \frac{\omega_2}{c} \left(1 - \frac{\epsilon_{xx} - \epsilon_{zz}}{\epsilon_{zz}} \sin^2 \theta_2 - \frac{\epsilon_{xz}}{\epsilon_{zz}} \sin 2\theta_2 \right) \approx n_{xx} \frac{\omega_2}{c}. \end{aligned} \quad (39)$$

For the polarizations we therefore have

$$p_{1y} = 1, \quad p_{2x} = \cos \theta_2 \approx 1, \quad p_{2z} = \sin \theta_2 \ll 1. \quad (40)$$

The solution of system (35) will be different depending on the sign of the product $k_{1z} k_{2z} \sim \cos \theta_1 \cos \theta_2$.

1) $\cos \theta_1 > 0, \cos \theta_2 > 0$.

In this case we naturally use the boundary conditions

$$A_1(0) = A_0, \quad A_2(0) = 0, \quad (41)$$

and accounting for these boundary conditions system (35) yields

$$\begin{aligned} A_1(z) &= A_0 \cos \kappa z, \\ A_2(z) &= \pm A_0 \frac{\kappa_{12}}{\kappa} \left(\frac{k_{1z}}{k_{2z}} \right)^{1/2} \sin \kappa z, \end{aligned} \quad (42)$$

where

$$\kappa = |\kappa_{12}| \approx \frac{\omega |\Delta \epsilon_{0yx}|}{4c n_{yy} n_{xx}}. \quad (43)$$

Here we account for Eqs. (34) and (37) as well as (39) and (40) as well as $\omega_2 \approx \omega_1 \equiv \omega$ [since $\Omega \ll \omega_1$ in Eq. (36)]; $\Delta \epsilon_{0yx}$ is taken from Eq. (38) subject to (18) and (19) (the terms with $\omega_{\alpha\beta}$ are discarded as small quantities).

It is possible to find the relative power contributed to

the diffracted wave (the diffraction efficiency) as the light propagates a distance d in the acoustic beam:

$$T = \frac{k_{2z}|A_2|^2}{k_{1z}|A_0|^2} = \sin^2 \kappa z |_{z=d}. \quad (44)$$

Equations (36)–(44) are applicable to both SBA as well as LBA with the only difference lying in the specific Bragg coherence conditions obtained from (36):

$$\text{(SBA)} \quad \begin{cases} 2k_1 \sin \theta_1 = -q \left(1 + \frac{k_1^2 - k_2^2}{q^2} \right), \\ 2k_2 \sin \theta_2 = q \left(1 - \frac{k_1^2 - k_2^2}{q^2} \right), \end{cases} \quad (45)$$

$$\text{(LBA)} \quad \begin{cases} 2k_1 \cos \theta_1 = -q \left(1 + \frac{k_1^2 - k_2^2}{q^2} \right), \\ 2k_2 \cos \theta_2 = q \left(1 - \frac{k_1^2 - k_2^2}{q^2} \right). \end{cases} \quad (46)$$

For SBA from (45) subject to (39) we have

$$\text{(SBA)} \quad \begin{cases} \sin \theta_1 = -\frac{\lambda_0}{2n_{yy}\Lambda} \left[1 - \left(\frac{\Lambda}{\lambda_0} \right)^2 (n_{xx}^2 - n_{yy}^2) \right], \\ \sin \theta_2 = \frac{\lambda_0}{2n_{xx}\Lambda} \left[1 + \left(\frac{\Lambda}{\lambda_0} \right)^2 (n_{xx}^2 - n_{yy}^2) \right]. \end{cases} \quad (47)$$

Depending on the sign of the difference $n_{xx}^2 - n_{yy}^2$, one of the Bragg angles $\theta_{1(2)}$ may be equal to zero; then for the second angle

$$\sin \theta_{2(1)} = \frac{\lambda_0}{n\Lambda}. \quad (48)$$

For LBA the simplest solution in Eq. (46) is $\cos \theta_1 = \cos \theta_2 = 1$, which corresponds to the minimum values of the wave vector and the acoustic frequency:

$$q_{min} = |k_2 - k_1|, \quad (49)$$

$$\Omega = \Omega_{min} = s_{(z\bar{t})} |k_2 - k_1| = \frac{2\pi}{\lambda_0} v_1 \left(1 - \frac{2B_{14}}{C_{44}} U_2 \right)^{1/2} |n_{xx} - n_{yy}|.$$

As we shall see below (Section 4) by virtue of the smallness of $|n_{xx} - n_{yy}|$ ($\lesssim 10^{-3}$) Eq. (49) yields too small a frequency Ω (too large a wavelength Λ) to satisfy condition (7) with reasonable sample dimensions. It does no good to change the direction of the incident beam by the small angle θ_1 for which

$$q \approx q_{min} / \cos \theta_1.$$

We recall that here we are considering the case $\cos \theta_1 \cos \theta_2 > 0$. The situation changes for the case $\cos \theta_1 \cos \theta_2 < 0$.

2) $\cos \theta_1 > 0, \cos \theta_2 < 0$.

In accordance with Fig. 2 such backscattering may occur only for LBA. The corresponding boundary conditions take the form

$$A_1(0) = A_0, \quad A_2(d) = 0,$$

for which Eqs. (35) yield

$$\text{(LBA)} \quad \begin{cases} A_1(z) = A_0 \frac{\text{ch } \kappa(d-z)}{\text{ch } \kappa d} \\ A_2(z) = \pm A_0 \frac{\kappa_{12}\omega_2}{\kappa\omega_1} \left| \frac{k_{1z}}{k_{2z}} \right|^{1/2} \frac{\text{sh } \kappa(d-z)}{\text{ch } \kappa d}. \end{cases} \quad (50)$$

The fraction of reflected light (for $z = 0$) is equal to

$$R = \left| \frac{k_{2z}}{k_{1z}} \right| \left| \frac{A_2(0)}{A_1(0)} \right|^2 \approx \text{th}^2 \kappa d.$$

In this situation we can consider the case $\cos \theta_1 = -\cos \theta_2 = 1$ corresponding to the maximum acoustic frequency

$$\Omega = \Omega_{max} = \frac{2\pi}{\lambda_0} v_1 \left(1 - \frac{2B_{14}}{C_{44}} U_2 \right)^{1/2} (n_{xx} + n_{yy}). \quad (51)$$

However this yields such high hypersonic frequencies ($\approx 10^{11} \text{ s}^{-1}$) that, generally speaking, condition (14) is violated. The frequency Ω_{max} may be decreased to some degree (by a few tenths) as a result of multiplication with U_2 in (51).

Version B. In considering version B for which the coordinate axes in Fig. 2 are indicated in braces we easily observe that the corresponding equations can be obtained from the equations of version A by the cyclic substitution

$$x \rightarrow z \rightarrow y \rightarrow x.$$

Specifically in place Eqs. (42), (43), (44), (47) and (49) of version A we have

$$A_1(y) = A_0 \cos \kappa y, \quad A_2(y) = \pm A_0 \frac{\kappa_{12}}{\kappa} \left(\frac{k_{1y}}{k_{2y}} \right)^{1/2} \sin \kappa y, \quad (42')$$

$$\kappa = |\kappa_{12}| = \frac{\omega |\Delta \epsilon_{0zz}|}{4C n_{xx} n_{zz}} \quad (43')$$

$$T = \frac{k_{2y}}{k_{1y}} \left| \frac{A_2}{A_0} \right|^2 = \sin^2 \kappa y |_{y=d}, \quad (44')$$

$$\text{(SBA)} \quad \begin{cases} \sin \theta_1 = -\frac{\lambda_0}{2n_{xx}\Lambda} \left[1 - \left(\frac{\Lambda}{\lambda_0} \right)^2 (n_{zz}^2 - n_{xx}^2) \right], \\ \sin \theta_2 = \frac{\lambda_0}{2n_{zz}\Lambda} \left[1 + \left(\frac{\Lambda}{\lambda_0} \right)^2 (n_{zz}^2 - n_{xx}^2) \right]. \end{cases} \quad (47')$$

In place of (49) for $\sin 3\varphi_H = 0$ for the normal mode with $u \parallel X$ we find

$$\Omega_{min} = \frac{2\pi}{\lambda_0} v_2 \left(1 - \frac{B_{66}}{C_{66}} U_1 \right)^{1/2} |n_{zz} - n_{xx}|. \quad (49')$$

4. DISCUSSION OF RESULTS WITH APPLICATION TO Fe_2O_3 AND FeBO_3

Ordinarily in characterizing the acoustooptic properties of a material the acoustooptic Q tensor^{1,2}

$$M_{\alpha\beta\gamma\delta} = \frac{|P_{\alpha\beta\gamma\delta}|^2}{n_{\alpha\alpha} n_{\beta\beta} \rho s_{(\gamma\delta)}^3} \quad (52)$$

is used. If we define the acoustic intensity (the acoustic power density) corresponding to the component $e_{\gamma\delta}$ as

$$I_{\text{ab}} = 4\rho s_{(\gamma\delta)}^2 \overline{e_{\gamma\delta}^2} = 2\rho s_{(\gamma\delta)}^2 e_{0\gamma\delta}^2,$$

the acoustooptic coupling constant κ , Eqs. (37), (43) is written through \hat{M} and I_s as

$$\kappa = (\pi/\lambda_0) (MI_{s0}/2)^{1/2}. \quad (53)$$

We evaluate κ for $I_s = 1 \text{ W/cm}^2$ as an example in all cases below (the conversion to the other power level is trivial). Using the known values of the components of tensor \hat{P} from the table we carry out quantitative estimates of the param-

eters \hat{M} and κ which determine the diffraction efficiencies (44), (44') for specific cases of Fe_2O_3 and FeBO_3 . We focus solely on normal acoustical modes with velocities (30) and (31) for the sound. Without going into details, it is necessary to specify in each case the limits on their frequencies imposed by conditions (7) and (34). Without going into detail we note that for SBA condition (7) is stronger for version A and yields $\Omega/2\pi \geq d^{-1/2} \cdot 10^2$ MHz (where d is a number equal to the wafer thickness in cm), while condition (34) is stronger for version B and yields the very high frequencies of $\Omega/2\pi \geq 10^3$ MHz. In the LBA case the frequencies Ω_{min} are evaluated from Eqs. (49) and (49').

Given below are results from the quantitative estimates of \hat{M} (in units of $10^{-15} \text{ kg}^{-1} \cdot \text{s}^3$) and κ (cm^{-1}) for a number of specific cases.

1) SBA, version A: $\mathbf{k}_1, \mathbf{k}_2 \parallel \mathbf{Z}$ (approximate), $\mathbf{p}_1 \parallel \mathbf{Y}$, $\mathbf{p}_2 \parallel \mathbf{X}$ (approximate).

a) $\cos 3\varphi_H = 0$, $\mathbf{q} \parallel \mathbf{X}$, $\mathbf{u} \parallel \mathbf{Y}$. Here we are dealing with diffraction by a normal acoustical mode with a phase velocity $s_{(xy)}$ (31). Here

$$M \equiv M_{(xy)(xy)} = \begin{cases} 2,5; \kappa=0,10 & (\alpha\text{-Fe}_2\text{O}_3), \\ 1,0; \kappa=0,14 & (\text{FeBO}_3). \end{cases} \quad (54)$$

b) $\sin 3\varphi_H = 0$, $\mathbf{q} \parallel \mathbf{X}$, $\mathbf{u} \perp \mathbf{X}$. Here oscillations with $\mathbf{u} \parallel \mathbf{Y}$ and $\mathbf{u} \parallel \mathbf{Z}$ are mixed into two transverse modes. The mode in which the $\mathbf{u} \parallel \mathbf{Z}$ displacement predominates is preferred, since the acoustic Q -factor corresponding to it $M_{(xy)(xz)} > M_{(xy)(xy)}$ (54). Indeed

$$M \equiv M_{(xy)(xz)} = M_{(xy)(xz)} = \begin{cases} 52; \kappa=0,44 & (\alpha\text{-Fe}_2\text{O}_3), \\ 13; \kappa=0,49 & (\text{FeBO}_3). \end{cases} \quad (55)$$

Without providing the explicit forms of the equations for the velocities and polarizations (u_x/u_z) for these modes we simply note that like the effective elasticity moduli $C_{44}^*(H)$, $C_{66}^*(H)$ and $C_{14}^*(H)$ that define these quantities they become dependent on H due to magnetoelastic interaction. For hematite this is particularly true of the quantity C_{14} which grows by a factor of 1.5 (for $H = 1$ kOe). The mode mixing noted here is related specifically to this quantity. (The quantity $C_{14}(H)$ drops by 25–50% for FeBO_3 .)

The situation $\theta_1 = 0$ in accordance with (47) may also occur for both these cases [since $n_{xx}^2 - n_{yy}^2 > 0$], for which we find the approximately identical quantity of $\theta_2 \approx 0.7^\circ$ from (48) for both antiferromagnets. The acoustic frequencies required for this case

$$\Omega = (2\pi/\lambda_0) s_{(xz)} (n_{xx}^2 - n_{yy}^2)^{1/2}$$

depend on the mode type. In the case $\mathbf{u} \approx \parallel \mathbf{Z}$ we have $\Omega/2\pi = 100$ MHz for $\alpha\text{-Fe}_2\text{O}_3$ and $\Omega/2\pi = 250$ MHz for FeBO_3 , while for $\mathbf{u} \parallel \mathbf{X}$ we have $\Omega/2\pi = 180$ MHz for $\alpha\text{-Fe}_2\text{O}_3$ and $\Omega/2\pi = 417$ MHz for FeBO_3 .

The smallness of the Bragg angle θ_2 in these cases will not hinder the experiment since the diffracted and incident beams are depolarized by $\pi/2$.

2) SBA version B: $\mathbf{k}_1, \mathbf{k}_2 \parallel \mathbf{Y}$ (approximate), $\mathbf{p}_1 \parallel \mathbf{X}$, $\mathbf{p}_2 \parallel \mathbf{Z}$ (approximate).

Since we have $\mathbf{q} \parallel \mathbf{Z}$, the optimum diffraction efficiency will be provided by sound with $\mathbf{u} \parallel \hat{\xi}$: a normal acoustic mode of velocity $s_{(z\xi)}$, given by (30). In this case the data provided in the table permit estimates only for FeBO_3 :

$$M_{[xz](z\xi)} = 22,4, \kappa = 0,65. \quad (56)$$

Yet this still does not provide the total diffraction efficiency since we have $P_{xz(z\xi)} = P_{(xz)(z\xi)} + P_{[xz](z\xi)}$, while the first term ($\sim \Pi_2$) is still unknown.

Returning to Eqs. (47') we see that since $n_{xx} \approx n_0 > n_{zz} \approx n_e$ holds for FeBO_3 , the situation $\sin \theta_2 = 0$ is possible for

$$\pm \sin \theta_1 \approx -\frac{\lambda_0}{n_0 \Lambda} = -\left(1 - \frac{n_e^2}{n_0^2}\right)^{1/2}, \quad \frac{\Omega}{2\pi} = \frac{s_{(z\xi)}}{\lambda_0} (n_0^2 - n_e^2)^{1/2}.$$

This yields $\theta_1 \approx \pm 13^\circ$ and $\Omega/2\pi = 4.36$ GHz.

This version can be altered by transposing the X and Z axes (more precisely, by carrying out the substitution $z \rightarrow x$ and $x \rightarrow -z$ in all equations of version B). Here in order to assure that the sound remains a normal mode [with $\mathbf{q} \parallel \mathbf{X}$, $\mathbf{u} \parallel \mathbf{Y}$ and velocity $s_{(xy)}$ (31)] we can set $\cos 3\varphi_H = 0$. The corresponding values of \hat{M} and κ are equal to

$$M_{[xz](xy)} = 4,9, \kappa = 0,3. \quad (57)$$

Since n_{xx} and n_{zz} have been transposed in Eqs. (47'), we now have $\theta_1 = 0$, while $\theta_2 = \pm 13^\circ$. However the acoustic mode velocity has changed and this now corresponds to a different frequency: $\Omega/2\pi \approx 8$ GHz.

3) LBA, version A: $\mathbf{k}_1 \parallel \mathbf{k}_2 \parallel \mathbf{q} \parallel \mathbf{Z}$, $\mathbf{p}_1 \parallel \mathbf{Y}$, $\mathbf{p}_2 \parallel \mathbf{X}$.

We again have the highest diffraction efficiency for $\mathbf{u} \parallel \hat{\xi}$. The values of \hat{M} and κ coincide with those from (55). The acoustic frequency given by Eqs. (49) is $\Omega_{min} = 0.6$ and 1.3 MHz for $\alpha \equiv \text{Fe}_2\text{O}_3$ and FeBO_3 , respectively. Unfortunately at these frequencies condition (7) requires entirely unrealistic sample dimensions ($d > 10^3$ cm).

4) LBA, version B ($\sin 3\varphi_H = 0$): $\mathbf{k}_1 \parallel \mathbf{k}_2 \parallel \mathbf{q} \parallel \mathbf{Y}$, $\mathbf{p}_1 \parallel \mathbf{X}$, $\mathbf{p}_2 \parallel \mathbf{Z}$.

Using a normal acoustic mode with $\mathbf{u} \parallel \mathbf{X}$ we obtain M and κ that coincide with (57); in this case the acoustic frequency in accordance with (49') is $\Omega_{min} = 680$ MHz (for FeBO_3). The required dimensions of the sample to satisfy Bragg conditions (7) are $d > 10^{-2}$ cm.

Quantitative estimates of the parameter κ which defines diffraction efficiency (44), (44') have been given only for individual geometrical situations, since this is permitted by the available experimental data. Moreover in order to avoid cumbersome calculations we have largely limited the analysis to the simplest normal acoustical modes (for which the polarization vectors lie along the coordinate axes) although when necessary it is easy to carry out calculations for modes with other polarizations.

It is clear from these examples that if we wish to limit light diffraction to sound of the lowest possible frequency (hundreds of megahertz) the SBA case, version A should be selected. Here it is possible to achieve a diffraction efficiency of tens of percent for samples of dimensions $d \approx 1$ cm at acoustic power levels of the order of 1 W/cm^2 . However millimeter-sized samples (which are available in a number of laboratories around the country) and lower acoustic power levels are sufficient for detecting the effect.

Version B (both the SBA and LBA cases) requires somewhat higher acoustic frequencies $\Omega/2\pi \geq 10^3$ MHz, although the diffraction efficiency (at an identical acoustic power level) may be noticeably larger for this case.

It is important to point out that there are more favorable geometrical situations for experimental purposes. How-

ever in order to estimate the magnitude of the effect for these situations it is necessary to know the other components of the tensor $\varepsilon_{\alpha\beta}^L$ in addition to those given in the Appendix. It is therefore extremely important to carry out magneto-optic measurements prior to implementing experiments on anti-ferromagnetic light diffraction by sound. Ideally it would be desirable to measure all components in (17) and (18). This is particularly true of iron borate which is transparent in the visible range.

We note in conclusion that in antiferromagnets (as in ferromagnets)¹² the acoustical waves whose diffraction was examined above are in fact coupled magnetoelastic waves and under certain conditions can be excited by an isolated uniform magnetic field of the same frequency.

The values of constants used in the paper for quantitative estimates. Room temperature range (the experimental spread of value is not accounted for). The data are from Refs. 6–9, 11, 13–18.

Hemitite ($\alpha\text{-Fe}_2\text{O}_3$). $\rho = 5.29 \text{ g/cm}^3$,
 $2C_{66} = C_{11} - C_{12} = 18.7 \cdot 10^{11} \text{ erg/cm}^3$, $C_{44} = 8.5 \cdot 10^{11} \text{ erg/cm}^3$, $M_0 = 870 \text{ G}$, $H_E = 9.2 \cdot 10^6 \text{ Oe}$, $H_D = 22 \cdot 10^3 \text{ Oe}$,
 $H_\Delta^2 = 13 \cdot 10^6 \text{ Oe}^2$, $B_{66} = B_{11} - B_{12} = 8 \cdot 10^6 \text{ erg/cm}^3$,
 $2B_{14} = 27 \cdot 10^6 \text{ erg/cm}^3$, $n_{xx} \approx n_{yy} \approx n_0 = 2.84$;
 $n_{zz} \approx n_e = 2.64$, $n_{xx}^2 - n_{yy}^2 = 12 \cdot 10^{-4}$, $C_{14} = -1.3 \cdot 10^{11} \text{ erg/cm}^3$.

Iron borate (FeBO_3). $\rho = 4.28 \text{ g/cm}^3$,
 $2C_{66} = C_{11} - C_{12} = 30 \cdot 10^{11} \text{ erg/cm}^3$, $C_{44} = 9.5 \cdot 10^{11} \text{ erg/cm}^3$, $M_0 = 560 \text{ G}$, $H_E = 2.6 \cdot 10^6 \text{ Oe}$, $H_D = 66 \cdot 10^3 \text{ Oe}$,
 $H_\Delta^2 = 1 \cdot 10^6 \text{ Oe}^2$, $B_{66} = B_{11} - B_{12} = 5.2 \cdot 10^6 \text{ erg/cm}^3$,
 $2B_{14} = 12.7 \cdot 10^6 \text{ erg/cm}^3$, $n_{xx} \approx n_{yy} \approx n_0 = 2.241$,
 $n_{zz} \approx n_e = 2.184$, $\varepsilon_{[yz]}^L/i = a = 14 \cdot 10^{-4}$, $n_{xx}^2 - n_{yy}^2 = 6.6 \cdot 10^{-4}$, $C_{14} = 2 \cdot 10^{11} \text{ erg/cm}^3$.

- ¹A. Yariv and P. Yeh, *Optical Waves in Crystals*, Wiley, New York (1984).
- ²E. D'aleon and D. Ruaye, *Elastic Waves in Solids* (Nauka Press, Moscow, 1982).
- ³G. A. Smolenskii, R. V. Pisarev and I. G. Siniĭ, *Usp. Fiz. Nauk.* **116**, 231 (1975) [*Sov. Phys. Usp.* **18**, 410 (1975)].
- ⁴E. A. Turov, *Kinetics, Optical and Acoustical Properties of Antiferromagnets*. Sverdlovsk: Ural Division of the USSR Academy of Sciences, 1990.
- ⁵N. I. Evtikheev, V. V. Moshkin, V. L. Preobrazhenskii and N. A. Ekonomov, *Pis'ma v ZhETF*, **35**, 31 (1982) [*JETP Lett.* **35**, 38 (1982)]; V. L. Preobrazhenskii, *Doctoral Dissertation in Physics and Mathematics* (MIREA, Moscow, 1986).
- ⁶A. S. Borovik-Romanov and E. G. Rudashevskii, *Ah. Eksp. Teor. Fiz.* **47**, 2095 (1964) [*Sov. Phys. JETP*, **20**, 407 (1964)].
- ⁷V. I. Ozhogin and V. L. Preobrazhenskii, *Zh. Eksp. Teor. Fiz.* **73**, 988 (1977) [*Sov. Phys. JETP*, **46**, 523 (1977)].
- ⁸Yu. M. Fedorov and A. A. Leksikov, *Pis'ma v ZhETF*, **27**, 389 (1978) [*JETP Lett.*, **27**, 365 (1978)].
- ⁹R. Wolfe, A. J. Kurtzig and R. C. LeCraw, *J. Appl. Phys.* **41** 1218 (1970).
- ¹⁰E. A. Turov, *Zh. Eksp. Teor. Fiz.* **96**, 2140 (1989) [*Sov. Phys. JETP*, **69**, 1211 (1989)].
- ¹¹M. H. Seavey, *Sol. State Comm.* **10**, 219 (1972).
- ¹²A. A. Lugovoy and E. A. Turov, *Zh. Eksp. Teor. Fiz.* **94**, 358 (1988) [*Sov. Phys. JETP*, **67**, 1291 (1988)].
- ¹³B. Ya. Kotyuzhanskii and L. A. Prozorova, *Zh. Eksp. Teor. Fiz.* **81**, 1913 (1981) [*Sov. Phys. JETP*, **54**, 1013 (1981)].
- ¹⁴L. V. Velikhov, A. S. Prokhorov, E. G. Rudashevskii and V. N. Seleznev, *Zh. Eksp. Teor. Fiz.* **66**, 1847 (1974) [*Sov. Phys. JETP* **66**, 909 (1974)].
- ¹⁵A. I. Pankrats, *Abstract of Dissertation for Candidates's Degree in Physics and Mathematics*. Novosibirsk: Institute of Physics, Siberian Division of the USSR Academy of Sciences, 1977.
- ¹⁶W. Jantz and W. Wettling, *Appl. Phys.* **15**, 339 (1978).
- ¹⁷W. Jantz, J. R. Sandercock and W. Wettling, *J. Phys.* **2231** (1976).
- ¹⁸V. S. Merkulov, E. G. Rudashevskii, A. Le Gall' and K. Leykyuras, *Zh. Eksp. Teor. Fiz.* **75**, 628 (1978) [*Sov. Phys. JETP*, **48**, 316 (1978)].

Translated by Kevin S. Hendzel